J. Biochem. **140**, 509–515 (2006)
doi:10.1093/jb/mvj179

Molecular Mechanisms of Improvement of Hydrolytic Antibody 6D9 by Site-Directed Mutagenesis

Naoko Takahashi-Ando[1,*,†], Kazuko Shimazaki[1,*], Hiroyuki Kakinuma[1,*], Ikuo Fujii[2,*] and Yoshisuke Nishi[1,*,†]

[1]Laboratory of Life Science & Biomolecular Engineering, Japan Tobacco, Inc. 6-2, Umegaoka, Aoba-ku, Yokohama, Kanagawa 227-8512; and [2]Department of Biological Science, Graduate School of Science, Osaka Prefecture University, 1-2, Gakuen-cho, Sakai, Osaka 599-8570

Received May 28, 2006; accepted August 15, 2006

We performed a series of site-directed mutagenesis experiments of catalytic antibody, 6D9, which hydrolyzes a prodrug of chloramphenicol, based on our previous directed evolution study [Takahashi *et al.* (2001) *Nat. Biotechnol.* 19, 563–567]. Since we previously found that the variants with a mutation of Ser(L27e)Tyr afforded a one order of magnitude increase in catalytic rate, we created a site-directed mutant containing this mutation. The resulting mutant, 6D9-Ser(L27e)Tyr, had 6.5-fold higher k_{cat}/k_{uncat} and 9.8-fold higher k_{cat}/K_m than wild-type 6D9. We also created 6D9-Thr(L27a)Pro, since this mutation occurred frequently in the previous directed evolution, and it had 2.1-fold higher k_{cat}/k_{uncat} and k_{cat}/K_m than 6D9. Kinetic and computational analyses suggest that Tyr at L27e contributes to transition-state stabilization, while Pro at L27a does not interact with the transition-state structure directly, but obviously contributes to enhanced catalytic activity. Including double mutants that combined favourable substitutions, we created seven site-directed mutants. However, none of them had higher catalytic activities than some of highly improved variants obtained in the previous directed evolution. The present study gives direct evidence that not only a specific amino acid residue which obviously contributes to transition-state stabilization, but also a group of amino acid residues working in concert is important for efficient catalysis of a given transformation.

Key words: abzyme, antibody engineering, catalytic antibodies, computational analysis, molecular evolution.

Abbreviations: TSA, transition-state analog.

Catalytic antibody technology has gained increasing attention, because it has potentials to produce tailor-made catalysts for many chemical transformations (*1*, *2*) and for novel medical therapy (*3–5*). However, practical application of this technology has been hampered by the relatively low efficiency of catalytic antibodies as biocatalysts. To overcome this limitation, several methodologies have been proposed including reactive immunization, a bait-and-switch strategy and directed evolution (review in Ref. *6*). Previously, we succeeded in improving the catalytic activity of a pre-existing catalytic antibody by using a newly designed derivative of transition-state analog (TSA) in directed evolution.

As a starting material for directed evolution, we used 6D9, which hydrolyzes a prodrug of chlormaphenicol (Fig. 1) (*7*). A panel of catalytic antibodies including 6D9 was elicited by immunization of phosphonate TSA **3**, and kinetic studies have revealed that, except for 7C8, these antibodies catalyze the hydrolysis by the same basic mechanism of transition-state stabilization (*8*). The structural study and site-directed mutagenesis study of 6D9 strongly suggested that His(L27d) interacts with the TSA through a hydrogen bond and thus plays an essential role in transition-state stabilization (*9*, *10*).

In directed evolution of 6D9, we utilized TSA **3** and its derivative **4** for panning in the phage-display system (*11*). In TSA **4**, the strongly antigenic trifluoroacetyl group was replaced with an acetyl group, which was expected to emphasize the transition-state element, the tetrahedral phosphonate group. Six amino acid residues around His(L27d) were randomized and subjected to directed evolution. We succeeded in obtaining variants with highly improved catalytic activities from panning with TSA **4**, but not with TSA **3**. The kinetic, biochemical and modeling data are consistent with our hypothesis that the variants obtained from panning with TSA **4** better recognize the

*Present addresses: Naoko Takahashi-Ando, Plant & Microbial Metabolic Engineering Research Unit, RIKEN, 2-1, Hirosawa, Wako, Saitama 351-0198; Kazuko Shimazaki, Nippon Veterinary and Life Science University, Department of Veterinary, Laboratory of Structural Bioinformatics, 1-7-1, Kyonan-cho, Musashino, Tokyo 180-8602; Hiroyuki Kakinuma, Medicinal Chemistry Laboratory, Taisho Pharmaceutical CO., LTD., 1-403, Yoshino-cho, Saitama, Saitama 330-8530; Yoshisuke Nishi, Faculty of Bioscience, Nagahama Institute of Bio-Science and Technology, 1266 Tamura-cho, Nagahama, Shiga 526-0829.

†To whom correspondence should be addressed. Naoko Takahashi-Ando, Tel: +81-48-467-9796, E-mail: ntando@postman.riken.jp; Yoshisuke Nishi, Tel: +81-749-64-8122 (direct line)/+81-749-64-8100 (main line), Fax: +81-749-64-8140, E-mail: y_nishi@nagahama-i-bio.ac.jp

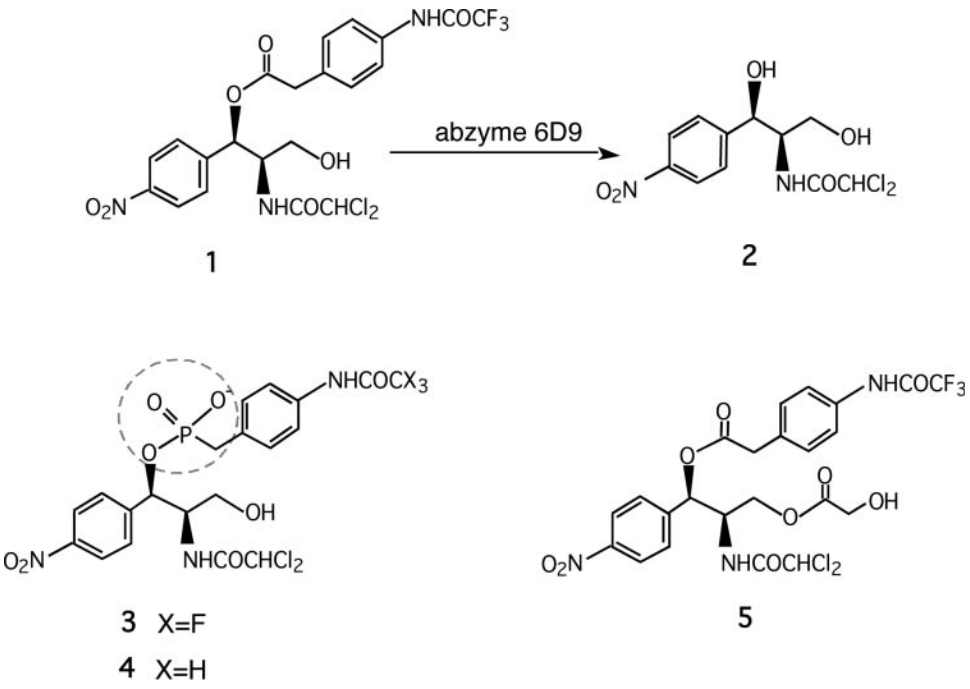

Fig. 1. **Chemical reaction catalyzed by abzyme, 6D9.** Chloramphenicol monoester derivative **1** was hydrolyzed by 6D9 to produce chloramphenicol **2**. The hapten **3** (X = F) is the transition state analog of hydrolysis of prodrug, and the hapten **4** (X = H) is a derivative of the hapten **3**. The substrate **5** was used for kinetic studies of IgGs and mutant Fabs.

transition-state element than those obtained from panning with TSA **3** (*12*).

In this study, we predicted some amino acid residues that contribute to increased catalytic activities of the highly evolved variants, and we performed a site-directed mutagenesis study so as to examine the roles of these amino acid residues. The kinetic and computational data provide insights into the molecular mechanisms of improvement of catalytic antibodies.

MATERIALS AND METHODS

Cloning of 6D9 and Other Related Antibodies—The V_H and κ gene fragments of catalytic antibodies, (6D9, 8C11, 4B5, 9C10, 3G6), were amplified by PCR as previously described (*13*). Amplified PCR products for each antibody were digested with *Spe*I–*Xho*I for V_H gene fragment and *Xba*I-*Sac*I for κ gene fragment, respectively, and were ligated into the pARA7 vector (*9*, *14*). Each of these ligates was transformed into *E. coli*, XL1-blue (Stratagene, Heidelberg, Germany) by electroporation.

Site-Directed Mutagenesis—Plasmids of site-directed mutants (see Table 1 for amino acid sequences) were produced using QuickChange Site-Directed Mutagenesis Kit (Stratagene) following the instructions provided by the manufacturer. For five single mutants of 6D9 [6D9-Ser(L27e)Tyr, 6D9-Ser(L27e)His, 6D9-Ser-(L27e)His, 6D9-Ser(L27e)Gly and 6D9-Thr(L27a)Pro], PCR was performed with 6D9 plasmid as a template using the following primers (mutated positions denoted in bold): Ser(L27e)Tyr mutagenic sense (5′-CAG ACC ATT GTA CAT **TA**T AAT GGA GAC ACG-3′), and antisense (5′-CGT GTC TCC ATT A**TA** ATG TAC AAT GGT CTG-3′); Ser(L27e)Arg mutagenic sense (5′-CAG ACC ATT GTA CAT **CG**T AAT GGA GAC ACG-3′), antisense (5′-CGT GTC TCC ATT A**CG** ATG TAC AAT GGT CTG-3′); Ser(L27e)His mutagenic sense (5′-CAG ACC ATT GTA CAT **CA**T AAT GGA GAC ACG-3′) and antisense (5′-CGT GTC TCC ATT A**TG** ATG TAC AAT GGT CTG-3′); Ser(L27e)Gly mutagenic sense (5′-CAG ACC ATT GTA CAT **G**GT AAT GGA GAC ACG-3′) and antisense (5′-CGT GTC TCC ATT AC**C** ATG TAC AAT GGT CTG-3′); Thr(L27a)Pro mutagenic sense (5′-AGA TCT AGT CAG **CC**G ATT GTA CAT-3′) and antisense (5′-ATG TAC AAT **C**G**G** CTG ACT AGA TCT-3′). For two double mutants of 6D9, 6D9-Thr(L37a)Pro/Ser(L27e)Tyr and 6D9-Thr(L37a)Pro/Ser(L27e)Arg, PCR was performed with 6D9-Ser(L27e)Tyr and 6D9-Ser(L27e)Arg as a template, respectively, with Thr(L27a)Pro mutagenic sense and antisense primers shown above. We also created a series of mutants containing Tyr at L27e from 6D9-related antibodies, 8D11, 4B5, 9C10 and 3G6 using the following primers: for 8D11-Asn(L27e)Tyr, mutagenic sense (5′-CAG ACC ATT GTA CAT **T**AT AAT GGA AAC ACC-3′) and antisense (5′-GGT GTT TCC ATT AT**A** ATG TAC AAT GGT CTG-3′); for 4B5-Ser(L27e)Tyr, mutagenic sense (5′-CAG ACC ATT GTA CAT **TA**T AAT GGA AAC ACC-3′) and antisense (5′-GGT GTT TCC ATT A**TA** ATG TAC AAT GGT CTG-3′); for 9C10-Ser(L27e)Tyr, mutagenic sense (5′-CAG AGC CTT GTA CAT **TA**T AGT GGA AAC ACC-3′) and antisense (5′-GGT GTT TCC ACT A**TA** ATG TAC AAG GCT CTG-3′); for 3G6-Ser(L27e)Tyr, mutagenic sense (5′-CAG AGC ATT GTG CAT **TA**T GAT GGA AAC ACC-3′) and antisense (5′-GGT GTT TCC ATC A**TA** ATG CAC AAT GCT CTG-3′). The nucleotide sequence was confirmed by using the PRISM Ready Reaction Dye Deoxy Terminator Cycle Sequencing Kit and a Model 377 DNA sequencer (Applied Biosystems, Foster City, CA). For antibody expression, these plasmids were transformed into MC1061 by electroporation.

Production and Purification of the Fab Fragments and IgG—For antibody expression, each plasmid was

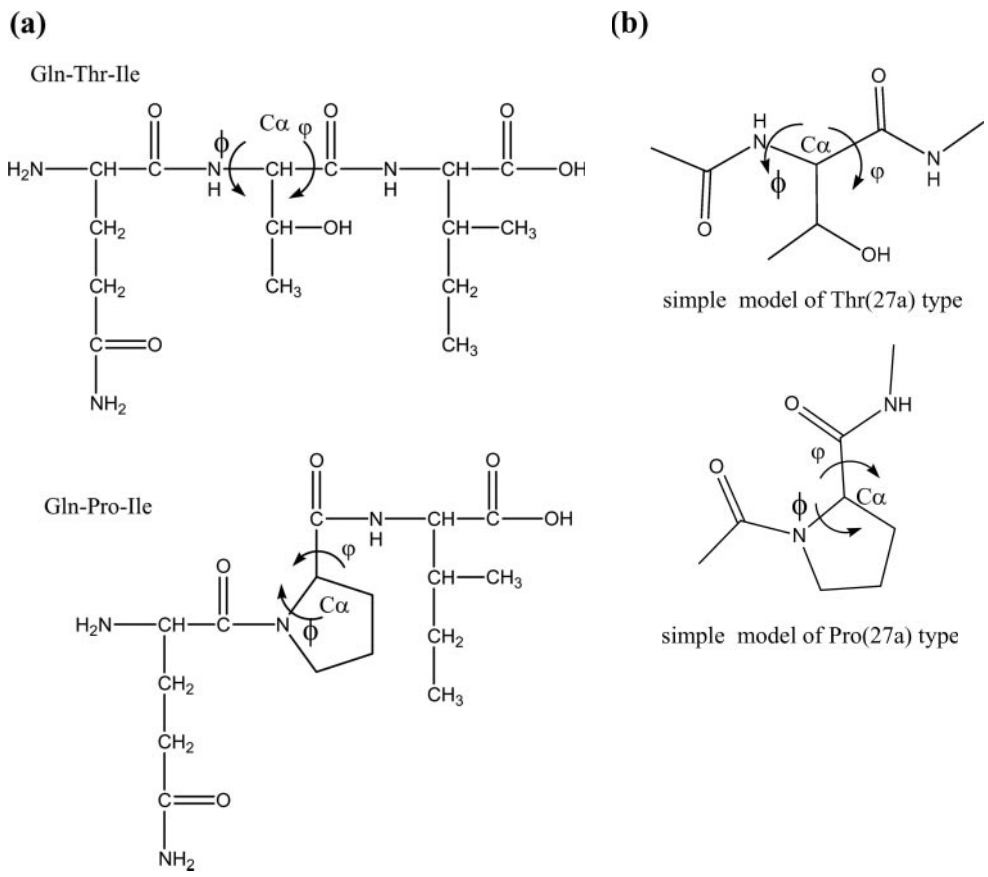

Fig. 2. **(a) Structures of tripeptides of Gln-Thr-Ile and Gln-Pro-Ile, (b) structures of simple models of Thr(27a) and Pro(27a) type.**

transformed into MC1061 (Invitrogen, Carlsbad, CA). Each transformant was incubated at 37°C in 2 liters of Cycle Grow medium (BIO101 Inc. La Jolla, CA) containing 100 μg/ml ampicillin. When OD_{600} of culture reached approx. 0.3, 2.0 g/liter of L-arabinose was added to induce Fab production. Cell culture was incubated for three days at 25°C before harvest. (We needed three days of incubation especially for site-directed mutants, since expression of these recombinant Fabs was very low.)

We purified the expressed Fabs as previously described with minor modifications (*12*). Filtered culture supernatant was concentrated using a Minitan Ultrafiltration system (Millipore, Bedford, MA), precipitated with ammonium sulfate at 65% saturation, and dialyzed against 10 mM phosphate buffer (pH 7.4). To fractionate the recombinant Fabs, a HiTrap Affinity column (Amersham Bioscience, Piscataway, NJ) coupled with affinity-purified anti-mouse IgG $F(ab')_2$ (Funakoshi, Tokyo) was used.

IgGs (6D9, 8C11, 4B5, 9C10, 3G6) were produced by hybridoma technology and purified as described previously (*8*).

Assay of Hydrolytic Activities—Kinetic parameters of catalytic antibodies (k_{cat}, K_m and K_i) were measured as described previously (*12*). Reaction was initiated by adding the substrate **5** to an antibody solution in 50 mM Tris-HCl buffer (pH 8.0), and carried out for 2 or 3 h at 25°C. The reaction mixture was applied to a Shimadzu SCL-10A HPLC unit (Kyoto, Japan) using a C-18 reverse phase column (YMC Co. Ltd., Kyoto, Japan) with water/acetonitrile (50:50)/0.1% trifluoroacetic acid at a flow rate of 0.5 ml/min. The values of k_{cat} and K_m were determined by fitting the data to the Michaelis-Menten equation while K_i values for TSA **3** were determined by fitting the data to a Henderson plot (*15*), both using the computer program KALEIDAGRAPH (Synergy Software, Reading, PA).

Computational Analysis—To examine the conformational stability around L27a, conformational analyses were performed to the original tri-peptide [Gln(L26)-Thr(L27a)-Ile(L27b), Thr type] and the mutated tri-peptide [Gln(L26)-Pro(L27a)-Ile(L27b), Pro type]. Initial geometries of the dihedral angles around L27a (ϕ and ψ) was generated by CONFLEX (*16*) and optimized conformation were obtained by MM3 (*17–19*). The obtained stable conformers were classified into 5 clusters by the dihedral angles around L27a for original tri-peptide (Thr type), and 3 clusters for mutated tri-peptide (Pro type), respectively, and the dihedral angles around L27a (Fig. 2a) were compared with those of the X-ray structure (*10*). Based on the conformations of the clusters, simple models of the original and mutated tri-peptide were generated, whose Gln(L26) and Ile(L27b) were substituted by acyl functional group and by methylamino functional group, respectively (Fig. 2b). The *ab initio* single point energies of these simple models were calculated by HF/6-31G* level of Gaussian98 (*20*). On the basis of their energies, the Boltzmann population at 25°C was calculated.

RESULTS AND DISCUSSION

In the previous directed evolution, all the variants with remarkably improved k_{cat} had Tyr at L27e, and no variants that did not have Tyr at L27e exhibited such high k_{cat} (*12*).

Table 1. **Amino acid sequences of LCDR1 of the IgGs and their site-directed mutants.**

Antibodies	L27 CRD1														
	24	25	26	27	a	b	c	d	e	28	29	30	31	32	33
6D9	R	S	S	Q	T	I	V	H	S	N	G	D	T	Y	L
6D9-Ser(L27e)Tyr	R	S	S	Q	T	I	V	H	**Y**	N	G	D	T	Y	L
6D9-Ser(L27e)Arg	R	S	S	Q	T	I	V	H	**R**	N	G	D	T	Y	L
6D9-Ser(L27e)Gly	R	S	S	Q	T	I	V	H	**G**	N	G	D	T	Y	L
6D9-Ser(L27e)His	R	S	S	Q	T	I	V	H	**H**	N	G	D	T	Y	L
6D9-Thr(L27a)Pro	R	S	S	Q	**P**	I	V	H	S	N	G	D	T	Y	L
6D9-Thr(L27a)Pro/Ser(L27e)Arg	R	S	S	Q	**P**	I	V	H	**R**	N	G	D	T	Y	L
6D9-Thr(L27a)Pro/Ser(L27e)Tyr	R	S	S	Q	**P**	I	V	H	**Y**	N	G	D	T	Y	L
8Hg*	R	S	S	Q	**P**	I	V	H	**Y**	N	G	D	**I**	Y	L
8D11	R	S	S	Q	T	I	V	H	N	N	G	N	T	Y	L
8D11-Asn(L27e)Tyr	R	S	S	Q	T	I	V	H	**Y**	N	G	N	T	Y	L
4B5	R	S	S	Q	T	I	V	H	S	N	G	N	T	Y	L
4B5-Ser(L27e)Tyr	R	S	S	Q	T	I	V	H	**Y**	N	G	N	T	Y	L
9C10	R	S	S	Q	S	L	V	H	S	S	G	N	T	Y	L
9C10-Ser(L27e)Tyr	R	S	S	Q	S	L	V	H	**Y**	S	G	N	T	Y	L
3G6	R	S	S	Q	S	I	V	Y	S	D	G	N	T	Y	L
3G6-Ser(L27e)Tyr	R	S	S	Q	S	I	V	Y	**Y**	D	G	N	T	Y	L

Bold letters indicate amino acid residues that were mutated by site-directed mutagenesis or directed evolution. *8Hg was made in our previous study (*11*, *12*).

Table 2. **Catalytic activities of 6D9 and its site-directed mutants.**

	k_{cat} (min^{-1})	K_m (μM)	k_{cat}/k_{uncat}	k_{cat}/K_m	K_i (nM)	K_m/K_i
6D9	0.129 ± 0.006	61.4 ± 8.4	935	2,101	68.5	895
6D9-Ser(L27e)Tyr	0.843 ± 0.022	41.1 ± 3.2	6,110	20,561	9.5	4,328
6D9-Ser(L27e)Arg	0.349 ± 0.009	57.1 ± 4.3	2,529	8,512	31.6	1,807
6D9-Ser(L27e)Gly	0.158 ± 0.011	44.3 ± 10.8	1,145	3,567	71.7	618
6D9-Ser(L27e)His	0.131 ± 0.005	42.4 ± 5.2	949	3,090	46.3	916
6D9-Thr(L27a)Pro	0.272 ± 0.005	60.8 ± 3.2	1,971	4,474	60.2	1,010
6D9-Thr(L27a)Pro/Ser(L27e)Arg	0.445 ± 0.015	81.2 ± 6.9	3,225	5,494	30.9	2,628
6D9-Thr(L27a)Pro/Ser(L27e)Tyr	1.200 ± 0.056	78.5 ± 8.8	8,696	15,287	7.2	10,896
8Hg*	2.593 ± 0.152	283.5 ± 31.0	18,791	9,146	10.2	27,794

*The data of 8Hg was from our previous study (*11*, *12*).

A three-dimensional molecular model of the complex of TSA **3** and the variant 8Hf, which had a 17.5-fold higher k_{cat} than that of 6D9, was constructed on the X-ray structure of a hapten-6D9 complex, and it showed that Tyr at L27e is positioned close to the phosphonate moiety of the hapten to form a hydrogen bond (*11*). Taken together, these results strongly suggest that Tyr at L27e played a crucial role in enhancing k_{cat}. Thus, we created a site-directed mutant, 6D9-Ser(L27e)Tyr. The Ser(L27e)Tyr mutation caused a 6.5-fold increase of k_{cat} and a 9.8-fold increase of k_{cat}/K_m (Table 2). The K_i value for TSA **3** of this mutant caused a 7.2-fold decrease, which indicated its higher affinity for TSA **3** and the transition-state structure than wild type 6D9.

In the directed evolution of 6D9, we obtained variants in which Ser at L27e was replaced by Arg, at an unexpectedly high frequency; after 8 rounds of panning with TSA **3** and **4**, the rates of variants with Ser(L27e)Arg were 35% and 64%, respectively. Thus, we hypothesized that Arg at L27e contribute to transition-state stabilization, although the variants with this mutation did not have highly improved catalytic activities. To test our hypothesis, we created 6D9-Ser(L27e)Arg, and found out that this mutant had a 2.7-fold higher k_{cat}/k_{uncat}, a 4.1-fold higher k_{cat}/K_m and a 2.2-fold lower K_i than 6D9. This result suggested that Arg at L27e also contributed to transition-state stabilization, although its effect was less than that of Tyr at L27e. We also created two single mutants, 6D9-Ser(L27e)Gly and 6D9-Ser(L27e)His. However, the kinetic parameters of both mutants were not significantly different from that of wild type, suggesting that these mutations did not have any effect on transition state stabilization.

We also created 6D9-Thr(L27a)Pro, since the Thr(L27a)Pro mutation was frequently found in our previous directed evolution using both TSA **3** and **4** (*12*). Replacement of Thr at L27a with Pro caused a 2.1-fold increase in k_{cat}. However, K_i for TSA **3** of this mutant was not significantly different from that of the wild type, suggesting that the affinity of this mutant for the transition-state structure did not improve. Thus, the modest increase of k_{cat} was not due to transition-state stabilization. We also created two double mutants containing two favorable mutations, 6D9-Thr(L27a)Pro/Ser(L27e)Tyr and 6D9-Thr(L27a)Pro/Ser(L27e)Arg, and performed kinetic studies. Like the single mutant, 6D9-Thr(L27a)Pro, these double mutants had modestly improved k_{cat} values and similar K_i values

Table 3. **Catalytic activities of the original IgGs and their L27eY mutants.**

	k_{cat} (min^{-1})	K_m (μM)	k_{cat}/k_{uncat}	k_{cat}/K_m	K_i (nM)	K_m/K_i
6D9 IgG	0.133 ± 0.006	56.5 ± 8.1	960	2,345	66.9	845
6D9 Fab	0.129 ± 0.006	61.4 ± 8.4	935	2,101	68.5	895
6D9-Ser(L27e)Tyr Fab	0.843 ± 0.022	41.1 ± 3.2	6,109	20,501	9.5	4,328
8D11 IgG	0.034 ± 0.017	2.62 ± 0.63	246	12,977	19.9	132
8D11-Asn(L27e)Tyr Fab	0.121 ± 0.004	1.29 ± 0.02	877	93,798	4.1	315
4B5 IgG	0.032 ± 0.001	3.73 ± 0.30	231	8,534	17.4	214
4B5-Ser(L27e)Tyr Fab	0.096 ± 0.003	1.99 ± 0.21	696	48,241	11.0	181
9C10 IgG	0.0077 ± 0.0008	0.71 ± 0.19	56	10,845	14.3	50
9C10-Ser(L27e)Tyr Fab	0.0137 ± 0.0007	0.37 ± 0.06	101	37,838	3.5	106
3G6 IgG	0.0065 ± 0.0003	1.31 ± 0.23	47	4,943	42.5	31
3G6-Ser(L27e)Tyr Fab	0.0142 ± 0.0005	2.42 ± 0.25	99	5,620	28.7	84

compared with their corresponding single mutants, 6D9-Ser(L27e)Tyr and 6D9-Ser(L27e)Arg. Based on the kinetic data, the effect of two mutations in 6D9-Thr(L27a)Pro/Ser(L27e)Tyr was additive. These observations suggested that the Thr(L27a)Pro mutation contributed to the increase in k_{cat}, although this improvement was not due to transition-state stabilization.

According to the crystal structure of 6D9, Thr at L27a did not have any direct contact with the TSA (*10*). A three-dimensional molecular model of TSA **3**-8Hf, one of the highly improved variants obtained from directed evolution, showed that Pro at L27a was also located away from the TSA (*11*). These structural studies did not contradict the results of the kinetic study, which suggests that Pro at L27a did not contribute directly to transition-state stabilization.

Nevertheless, in our directed evolution, the variants with Pro at L27a were obtained at an unexpectedly high rate. Thus, we hypothesized that, compared with Thr(L27a), Pro(L27a) plays an important role in the conformational stability. In order to verify the role of these residues from a structural point of view, the dihedral angles (ϕ, φ) of "Glu-Thr-Ile" (Thr type) for 6D9 and "Glu-Pro-Ile" (Pro type) for the variants were analyzed, based on the stable conformers obtained by CONFLEX/MM3 calculation. In the Thr type, five major conformation clusters (Thr-C1, Thr-C2, Thr-C3, Thr-C4 and Thr-C5) were obtained around the dihedral angles, whose averaged dihedral angles were Thr-C1 (–108.8°, 165.8°), Thr-C2 (–66.7°, 78.5°), Thr-C3 (–96.0°, –122.7°), Thr-C4 (–96.5°, –47.5°) and Thr-C5 (55.9°, –129.8°). On the other hand, in the Pro type, three conformation clusters (Pro-C1, Pro-C2 and Pro-C3) were obtained around the dihedral angles, whose averaged dihedral angles were Pro-C1 (–72.5°, 14.6°), Pro-C2 (–68.3°, 153.5°) and Pro-C3 (35.7°, 30.5°). Next, to examine which is the most stable cluster in Thr type or in Pro type, a simple model of each cluster was generated with those averaged dihedral angles, and single point energy calculation of each simple model was performed by HF/6-31G* level. The most dominant simple model of the Thr type was Thr-C1 and that of the Pro type was Pro-C2. The Bolzmann populations of those dominant simple models at 25°C were 62.1% for Thr-C1 and 98.7% for Pro-C2, respectively. The conformation of the Pro-C2 cluster, having the average dihedral angles around Pro(L27a) of –68.3° and 153.5°, was close to that of X-ray structure (–57.4°, 142.6°), while none of the dominant conformations of the Thr types was close to that of X-ray structure. This suggests that, in the original sequence, the conformation around Thr(L27a) was constrained, and the replacement of Thr(L27a) with Pro resulted in giving a more stable structure around L27a. Thus, this replacement likely caused stabilization around this region, and even possibly had some effect on the periphery of the active site. In fact, it has been reported that amino acid residues at the periphery of the active site contribute to improve catalytic activities (*21*, *22*).

A panel of catalytic antibodies obtained by immunization with TSA **3**, excluding 7C8, followed the equation of transition-state theory ($k_{cat}/K_m = k_{uncat}/K_{TS} \approx k_{uncat}/K_{TSA}$), thus, these antibodies supposedly catalyze the reaction through the same basic mechanism, transition-state stabilization (*8*). We also mutated these antibodies by introducing Tyr at L27e and measured the kinetic constants. As shown in Table 3, all the site-directed mutants with Tyr at L27e, had significantly higher catalytic activities than their corresponding original antibodies. The lower K_i values for TSA **3** of these mutants than those of their corresponding wild types indicate their enhanced affinities for the transition-state structure, and it strongly suggests that even in these relatives of 6D9, the introduction of Tyr at L27e would contribute to transition-state stabilization. This means that the catalytic activities of these relatives were also enhanced by the effective mutation for 6D9, and such mutation can give us various catalytic antibodies with a wide range of K_m values.

The present results, together with our previous studies of 6D9, indicate the following. In 6D9, His at L27d is an active site in catalysis by forming a hydrogen bond with the transition-state structure, and the substitution of Ser with Tyr at L27e of 6D9 results in forming an additional hydrogen bond with transition-state structure, which causes an increase in the catalytic activity. The site-directed mutant, 6D9-Ser(L27e)Tyr exhibited a 6.5-fold increase in k_{cat}. However, this k_{cat} value is less impressive than that of some highly improved variants obtained from directed evolution. Therefore, other mutations in those variants also seem to play some roles in their enhanced catalytic activities. A Thr(L27a)Pro mutation also caused a modest improvement in the k_{cat} value, although this mutation by itself probably does not help to stabilize the transition-state structure. In addition, our previous study (*11*, *12*) and the present study suggested that the hydrophobic amino acid at L31 also contributed to increase catalytic

activities. 8Hg, one of the highly evolved variants obtained by panning, contained three mutations, Thr(L27a)Pro/Ser(L27e)Tyr/Thr(L31)Ile. Compared with 6D9-Thr(L27a)Pro/Ser(L27e)Tyr, 8Hg had two-fold k_{cat}, which was supposedly caused by decreasing affinity toward substrate (*11*). Taken together, these findings showed that some amino acid residues contribute to enhance catalytic activities through transition-state stabilization and other mechanisms, and several amino acid residues likely act in concert to increase catalytic activities.

Except for a few examples (*23*, *24*), it has been rather difficult to obtain mutants with enhanced catalytic activities by site-directed mutagenesis based on only kinetic and/or structural information (*25*). In this site-directed mutation study, however, we successfully created mutants with increased catalytic activities using the information of the directed evolution study. In the future, we can even obtain better variants by fixing such effective mutations as Ser(L27e)Tyr and Thr(L27a)Pro, and randomizing several amino acid residues for further directed evolution. A combination of directed evolution and site-directed mutagenesis may provide another way to acquire catalytic antibodies efficient enough for practical applications.

We greatly thank Ms. Kiyoe Suzuki for her excellent technical assistance. We also thank Ms. Yumiko Takaoka, Ms. Naoko Murakami, Ms. Fumiyo Saito, Ms. Keiko Shindo and Ms. Fukumi Kuratomi for their technical assistance. We are grateful to Dr. Lidong Liu, Dr. Kiyotaka Akiyama, and Dr. Yoshiko Aoki for their helpful suggestions and comments. This research was supported by the New Energy and Industrial Technology Development Organization as the R&D project of the Industrial Science and Technology Frontier Program.

REFERENCES

1. Hilvert, D. (2000) Critical analysis of antibody catalysis. *Annu. Rev. Biochem.* **69**, 751–793
2. Mundorff, E.C., Hanson, M.A., Varvak, A., Ulrich, H., Schultz, P.G., and Stevens, R.C. (2000) Conformational effects in biological catalysis: an antibody-catalyzed oxy-cope rearrangement. *Biochemistry* **39**, 627–632
3. Landry, D.W., Zhao, K., Yang, G.X., Glickman, M., and Georgiadis, T.M. (1993) Antibody-catalyzed degradation of cocaine. *Science* **259**, 1899–1901
4. Wentworth, P., Datta, A., Blakey, D., Boyle, T., Partridge, L.J., and Blackburn, G.M. (1996) Toward antibody-directed "abzyme" prodrug therapy, ADAPT: carbamate prodrug activation by a catalytic antibody and its in vitro application to human tumor cell killing. *Proc. Natl. Acad. Sci. USA* **93**, 799–803
5. Shabat, D., Rader, C., List, B., Lerner, R.A., and Barbas, C.F., III. (1999) Multiple event activation of a generic prodrug trigger by antibody catalysis. *Proc. Natl. Acad. Sci. USA* **96**, 6925–6930
6. Tanaka, F. (2002) Catalytic antibodies as designer proteases and esterases. *Chem. Rev.* **102**, 4885–4906
7. Miyashita, H., Karaki, Y., Kikuchi, M., and Fujii, I. (1993) Prodrug activation via catalytic antibodies. *Proc. Natl. Acad. Sci. USA* **90**, 5337–5340
8. Fujii, I., Tanaka, F., Miyashita, H., Tanimura, R., and Kinoshita, K. (1995) Correlation between Antigen-Combining-site structures and functions within a panel of catalytic antibodies generated against a single transition-state analog. *J. Am. Chem. Soc.* **117**, 6199–6209
9. Miyashita, H., Hara, T., Tanimura, R., Fukuyama, S., Cagnon, C., Kohara, A., and Fujii, I. (1997) Site-directed mutagenesis of active site contact residues in a hydrolytic abzyme: evidence for an essential histidine involved in transition state stabilization. *J. Mol. Biol.* **267**, 1247–1257
10. Kristensen, O., Vassylyev, D.G., Tanaka, F., Morikawa, K., and Fujii, I. (1998) A structural basis for transition-state stabilization in antibody-catalyzed hydrolysis: crystal structures of an abzyme at 1. 8 Å resolution. *J. Mol. Biol.* **281**, 501–511
11. Takahashi, N., Kakinuma, H., Liu, L., Nishi, Y., and Fujii, I. (2001) In vitro abzyme evolution to optimize antibody recognition for catalysis. *Nat. Biotechnol.* **19**, 563–567
12. Takahashi-Ando, N., Kakinuma, H., Fujii, I., and Nishi, Y. (2004) Directed evolution governed by controlling the molecular recognition between an abzyme and its haptenic transition-state analog. *J. Immunol. Meth.* **294**, 1–14
13. Huse, W.D., Sastry, L., Iverson, S.A., Kang, A.S., Alting-Mees, M., Burton, D.R., Benkovic, S.J., and Lerner, R.A. (1989) Generation of a large combinatorial library of the immunoglobulin repertoire in phage lambda. *Science* **246**, 1275–1281
14. Cagnon, C., Valverde, V., and Masson, J.M. (1991) A new family of sugar-inducible expression vectors for *Escherichia coli*. *Protein Eng.* **4**, 843–847
15. Angeles, T.S., Smith, R.G., Darsley, M.J., Sugasawara, R., Sanchez, R.I., Kenten, J., Schultz, P.G., and Martin, M.T. (1993) Isoabzymes: structurally and mechanistically similar catalytic antibodies from the same immunization. *Biochemistry* **32**, 12128–12135
16. Goto, H., and Osawa, E. (1993) An efficient algorithm for seaching low-energy conformers of cyclic and acyclic molecules. *J. Chem. Soc. Perkin Trans.* **2**, 187–198
17. Allinger, N.L., Yuh, Y.H., and Lii, J.-H. (1989) Molecular mechanics. The MM3 force field for hydrocarbons. 1. *J. Am. Chem. Soc.* **111**, 8551–8566
18. Lii, J.-H., and Allinger, N.L. (1989) Molecular mechanics. The MM3 force field for hydrocarbons. 2. Vibrational frequencies and thermodynamics. *J. Am. Chem. Soc.* **111**, 8566–8575
19. Lii, J.-H., and Allinger, N.L. (1989) Molecular mechanics. The MM3 force field for hydrocarbons. 3. The van der Waals' potentials and crystal data for aliphatic and aromatic hydrocarbons. *J. Am. Chem. Soc.* **111**, 8576–8582
20. Frisch, M.J., Trucks, G.W., Schlegel, H.B., Scuseria, G.E., Robb, M.A., Cheeseman, J.R., Zakrzewski, V.G., Montgomery Jr., J.A., Stratmann, R.E., Burant, J.C., Dapprich, S., Millam, J.M., Daniels, A.D., Kudin, K.N., Strain, M.C. Farkas, Ö., Tomasi, J., Barone, V., Cossi, M., Cammi, R., Mennucci, B., Pomelli, C., Adamo, C., Clifford, S., Ochterski, J., Petersson, G.A., Ayala, P.Y., Cui, Q., Morokuma, K., Salvador, P., Dannenberg, J.J., Malick, D.K., Rabuck, A.D., Raghavachari, K., Foresman, J.B., Cioslowski, J., Ortiz, J.V., Baboul, A.G., Stefanov, B.B., Liu, G., Liashenko, A., Piskorz, P., Komáromi, I., Gomperts, R., Martin, R.L., Fox, D.J., Keith, T., Al-Laham, M.A., Peng, C.Y., Nanayakkara, A., Challacombe, M., Gill, P.M.W., Johnson, B., Chen, W., Wong, M.W., Andres, J.L., Gonzalez, C., Head-Gordon, M., Replogle, E.S., and Pople, J.A. (1998) *Gaussian 98, Revision A11*, Gaussian, Inc., Pittsburgh, PA
21. Arkin, M.R., and Wells, J.A. (1998) Probing the importance of second sphere residues in an esterolytic antibody by phage display. *J. Mol. Biol.* **284**, 1083–1094
22. Ruzheinikov, S.N., Muranova, T.A., Sedelnikova, S.E., Partridge, L.J., Blackburn, G.M., Murray, I.A., Kakinuma, H., Takahashi-Ando, N., Shimazaki, K., Sun, J., Nishi, Y., and Rice, D.W. (2003) High-resolution crystal structure of the Fab-fragments of a family of mouse

catalytic antibodies with esterase activity. *J. Mol. Biol.* **332**, 423–435
23. Romesberg, F.E., and Schultz, P.G. (1999) A mutational study of a Diels-Alderase catalytic antibody. *Bioorg. Med. Chem. Lett.* **9**, 1741–1744
24. Zheng, L., Baumann, U., and Reymond, J.L. (2004) Molecular mechanism of enantioselective proton transfer to carbon in catalytic antibody 14D9. *Proc. Natl. Acad. Sci. USA* **101**, 3387–3392
25. Larsen, N.A., de Prada, P., Deng, S.X., Mittal, A., Braskett, M., Zhu, X., Wilson, I.A., and Landry, D.W. (2004) Crystallographic and biochemical analysis of cocaine-degrading antibody 15A10. *Biochemistry* **43**, 8067–8076